



PAC-1 and isatin derivatives are weak matrix metalloproteinase inhibitors

Stian Sjøli^{a,1}, Ann Iren Solli^a, Øyvind Akselsen^b, Yang Jiang^b, Eli Berg^a, Trond Vidar Hansen^b, Ingebrigt Sylte^a, Jan-Olof Winberg^{a,*}

^a Department of Medical Biology, Faculty of Health Sciences, UiT-The Arctic University of Norway, 9037 Tromsø, Norway

^b School of Pharmacy, Department of Pharmaceutical Chemistry, University of Oslo, PO Box 1068, N-0316 Oslo, Norway

ARTICLE INFO

Article history:

Received 15 April 2014

Received in revised form 7 July 2014

Accepted 14 July 2014

Available online 18 July 2014

Keywords:

Docking

Inhibition

Isatin derivatives

PAC-1

MMPs

ABSTRACT

Background: Dysregulation of apoptotic cell death is observed in a large number of pathological conditions. As caspases are central enzymes in the regulation of apoptosis, a large number of procaspase-activating compounds (PAC-1 derivatives) and inhibitors (isatin derivatives) have been developed. Matrix metalloproteinases (MMPs) have been shown to have a dual role in apoptosis. Hence compounds that either activate or inhibit caspases should ideally not affect MMPs. As many PAC-1 derivatives contain a zinc chelating *ortho*-hydroxy *N*-acyl hydrazone moiety and isatin derivatives has two carbonyl groups on the indole core, it was of interest to determine to which extent these compounds can inhibit MMPs.

Methods: Eight PAC-1 and five isatin derivatives were docked into MMP-9 and MMP-14. The same compounds were synthesized, characterized, purified and tested as inhibitors of MMP-9 and MMP-14, using fluorescence quenched peptide and biological substrates. Some of the compounds were also tested for fluorescence quenching.

Results: Molecular docking suggested that the different compounds can bind to the MMP active sites. However, kinetic studies showed that neither of these compounds was a strong MMP inhibitor. IC₅₀ values over 100 μM were obtained after the enzyme activities were corrected for quenching. These IC₅₀ values are far above the concentrations needed to activate or inhibit the caspases.

Conclusion: The use of PAC-1 and isatin derivatives against caspases should have little or no effect on the activity of MMPs.

General significance: Activators and inhibitors of caspases are important potential therapeutic agents for several diseases such as cancer, diabetes and neurodegenerative disorders.

© 2014 Elsevier B.V. All rights reserved.

1. Introduction

Programmed cell death such as apoptosis is important for normal development and homeostasis of multicellular higher organisms [1]. A defect apoptotic regulation may induce several types of diseases, including cancer, diabetes and neurodegenerative diseases [1]. A typical trait of cancer cells is resistance to apoptosis, while uncontrolled apoptotic death of nerve cells occurs in neurodegenerative diseases like Alzheimer [1–5].

Caspases are a family of intracellular cysteine proteinases involved in the regulation of apoptosis [5,6]. There are two pathways that induce apoptosis through a cascade of events, the intrinsic and the extrinsic pathway [3,5]. Both pathways converge on the activation of procaspase-3, -6

and -7 to active caspases [5,6]. These three caspases are regarded as “executioner” caspases and the regulation of their activity controls the apoptotic cell death. Therefore, many compounds have been developed, which are involved either in the activation of the procaspases or the inhibition of active caspases. The intracellular pool of unbound zinc ions keeps the latency of the caspases. Among the compounds developed to activate procaspases are various agents that chelate zinc in solution such as the PAC-1 (procaspase-activating compounds) derivatives [7–10]. The central motif in PAC-1 derivatives that chelates zinc is the *ortho*-hydroxy *N*-acyl hydrazone moiety. Several studies have shown a correlation between the ability of PAC-1 derivatives to activate procaspase-3 and the cytotoxicity against cancer cells lines [7–10]. PAC derivatives like PAC-1a (DADH) that lack the *ortho*-hydroxy group are unable to chelate zinc and hence cannot activate procaspases, resulting in low cytotoxicity against cancer cells [10,11]. Compounds that inhibit the activity of caspases have also been developed. One such group of inhibitors are the isatin derivatives, and several isatin 1,2,3-triazoles have been shown to be strong caspase-3 and -7 inhibitors with K_i values in the lower nM region [12–14].

Abbreviations: MMP, matrix metalloproteinase; PAC-1, procaspase-3 activating compound; ZBG, zinc binding group

* Corresponding author.

E-mail address: jan.o.winberg@uit.no (J.-O. Winberg).

¹ SS was a fellow of BioStruct, the Norwegian national graduate school of Structural biology.

Matrix metalloproteinases (MMPs) are a subfamily of zinc and calcium dependent enzymes which belong to the metzincin superfamily [15, 16]. All MMPs contain an N-terminal signal peptide directing them to the secretory pathway. Most of the MMPs are secreted from the cells as inactive proenzymes, while some are linked to the cell membrane either through a type I transmembrane domain or a glycosylphosphatidyl-inositol (GPI) moiety. Together the MMPs are able to degrade most extracellular matrix proteins; in addition, they can also process a large number of non-extracellular matrix proteins such as growth factors, cytokines, chemokines, cell receptors, serine proteinase inhibitors and other MMPs. These proteinases have been shown to be involved in development and maintenance processes as well as in several diseases including cancer, diabetes and neurodegenerative diseases. MMPs have been shown to have a dual role in disease where they either promote or prevent disease development [16–23]. MMPs are also involved in apoptosis where they either induce or prevent apoptotic cell death [23–34].

Since MMPs are important enzymes in homeostasis and have a dual role in apoptotic cell death, potential therapeutic agents that activate or inhibit caspases should ideally not affect the activity of MMPs. As the zinc ion at the active site of MMPs may interact with zinc chelating moieties, the present study investigates to which extent various PAC-1 and isatin derivatives inhibit active MMP-9 and MMP-14.

2. Materials and methods

2.1. Materials

TRIS and DMSO were from Merck (Darmstadt, Germany). EDTA was from Fluka (Buchs, Switzerland). Acrylamide, Coomassie Brilliant Blue G-250 and Triton X-100 were from BDH (Poole, UK). Phorbol 12-myristate 13-acetate (PMA), blue dextran, Hepes, Brij-35, alkaline phosphatase-conjugated antibodies, gelatin, trypsin and SBTI were purchased from Sigma (St Louis, MO, USA). Gelatin-Sepharose, Q-Sepharose, Sephadex G-50 (fine), Amplify and mouse monoclonal antibody against MMP-9 were from GE-Healthcare (Uppsala, Sweden) and polyclonal antibodies against TIMP-1 were from Chemicon International Inc. (Temecula, CA, USA). Unlabeled molecular weight standards and DC Protein assay kit were from Bio-Rad (Richmond, CA, USA). DQTM-gelatin, Magic Marker molecular weight standards and pre-casted polyacrylamide gels (NuPAGE Novex 4–12% Bis-Tris gels) for Western blotting were from Invitrogen (Carlsbad, CA, USA). Human MT1-MMP/MMP-14 (catalytic domain) was from Calbiochem (San Diego, CA, USA). McaPLGDpaAR was from R&D Systems, Inc. (Minneapolis, MN, USA). FITC-labeled gelatin was from Molecular Probes (Eugene, OR, USA) and McaPL-OH was from Bachem AG (Basel, Switzerland).

2.2. Biosynthesis, purification and activation of proMMP-9

The biosynthesis and purification of proMMP-9 from THP-1 cells were performed as described previously and the purified proMMP-9 was activated by trypsin [35,36]. Briefly, approximately 156 µg/ml proMMP-9 was activated with trypsin (31 µg/ml) for 10 min at 37 °C in 0.1 M Hepes pH 7.5, 0.005% Brij-35 and 10 mM CaCl₂. The activation and processing of MMP-9 were terminated by adding a 50 times excess of SBTI (1.5 mg/ml) in relation to trypsin, followed by 10 minute incubation at room temperature. As the trypsin treatment of proMMP-9 results in a balance between activation and degradation of the metalloproteinase, and that the final concentration of active MMP-9 has not been determined by active site titration, the assumed amount of active MMP-9 in the inhibition experiments is overestimated.

2.3. Determination of the kinetic coefficients and inhibitory strength

To determine the kinetic and inhibitor kinetic coefficients K_m , V_{max} and IC_{50} , initial rate experiments were performed using a Perkin

Elmer LS 50 Luminescence spectrometer and the FL WinLab Software Package (Perkin Elmer). The excitation and emission wavelengths used were as follows: for the fluorescence quenched MMP peptide substrate McaPLGDpaAR (λ_{ex} = 320 nm, λ_{em} = 405 nm, slit width = 10 nm) and for DQ-gelatin (λ_{ex} = 490 nm, λ_{em} = 520 nm, slit width = 10 nm). All assays were performed at 37 °C in an assay buffer of 0.1 M Hepes pH 7.5, 0.005% Brij-35, 10 mM CaCl₂. In all assays, a final DMSO concentration of 5% was used with McaPLGDpaAR and 1% with DQ-gelatin. The exception was in experiments where the effect of DMSO on the MMP-9 degradation of the two substrates was determined. In all cases the obtained results are based on at least two independent experiments and values are presented as mean \pm s.d.

2.3.1. K_m determination

Initial rates were determined with McaPLGDpaAR concentrations ranging from 0.5 to 10.0 µM; higher substrate concentrations resulted in quenching. The concentrations of DQ-gelatin ranged from 0.5 to 30 µg/ml (5–300 nM, based on a M_r of 100,000). The K_m value was calculated from non-linear regression of the Michaelis–Menten equation using the Enzyme kinetic module in Sigma Plot.

2.3.2. Inhibition experiments with a fixed concentration of PAC-1 and isatin derivatives

To determine whether the PAC-1 and isatin derivatives were strong or weak inhibitors of MMP-9 and MMP-14, initial rates were performed in an assay containing either 1.0 or 100 µM of the derivatives along with 5.0 µM McaPLGDpaAR substrate and 30 nM MMP-9 or 3 nM MMP-14 in assay buffer.

2.3.3. IC_{50} determination

To determine IC_{50} values for the various compounds, a fixed low concentration of McaPLGDpaAR (5.0 µM) was used for both MMP-9 (30 nM in assay) and MMP-14 (3 nM in assay) along with varying concentrations of potential inhibitor. A low fixed concentration of DQ-gelatin (4 µg/ml; 40 nM) was used for MMP-9 along with various concentrations of the PAC-1 derivatives 020B and 72A. Plots of v_i/v_0 against $[I]$ were used to determine the IC_{50} value where v_i and v_0 represent the initial rate activity in the presence and absence of inhibitor (I), respectively. The IC_{50} value was calculated from Eq. (1) using Graph Pad Prism 5.

$$v_i/v_0 = 1/(1 + ([I]/IC_{50})) \quad (1)$$

2.4. Quenching experiments

The various PAC-1 and isatin 1,2,3-triazole derivatives themselves showed a concentration dependent fluorescence at the wavelengths used for the McaPLGDpaAR substrate. In order to determine to which extent these derivatives could quench the time dependent enzymatic increase in the fluorescence product of the processed substrate, quenching experiments were performed as follows. The fluorescence (λ_{ex} = 320 nm, λ_{em} = 405 nm, slit width = 10 nm) for various concentrations of the fluorescent product of the substrate McaPLGDpaAR, McaPL-OH (0–120 nM) was determined in the absence and presence of various concentrations of the PAC-1 and isatin derivatives (0–300 µM). From primary plots of fluorescence against [McaPL-OH], a secondary plot was produced where the y-axis contains the ratio of the quenched to the unquenched slope from the primary plots (sl_q/sl_0 (%)) and the x-axis the concentration of a given PAC-1 and isatin derivative. The slope of these secondary plots gives the quenching constant (a_1). The quenching constant (a_1) for the various derivatives is presented as the relative decrease in fluorescence in % per µM derivative. This constant (a_1) for a given derivative is used to correct the inhibitory curves for quenching.

Tests were also performed in order to determine if the PAC-1 and isatin 1,2,3-triazole derivatives also quench the fluorescence generated from the degradation of DQ-gelatin. In these experiments FITC-labeled gelatin was used as surrogate for degraded DQ-gelatin and these tests were performed as follows. The fluorescence ($\lambda_{\text{ex}} = 490 \text{ nm}$, $\lambda_{\text{em}} = 520 \text{ nm}$, slit width = 10 nm) for various concentrations of FITC-gelatin (0, 1.0, 2.0 and 4.0 $\mu\text{g/ml}$) was determined in the absence and presence of 100 μM 020B, 72A, TZ5 and TZ8 respectively.

2.5. Docking

The inhibitors to be docked were drawn, hydrogenated and energy optimized in Maestro (version 9.0, Schrodinger, LLC, New York, NY, 2009). Ligprep (version 2.3, Schrodinger, LLC, New York, NY, 2009) was used to generate tautomeric and expected ionic forms of all the compounds at $\text{pH } 7.0 \pm 2.0$, using Epik (version 2.0, Schrodinger, LLC, New York, NY, 2009) with metal binding and default settings [37]. X-ray structures of MMP-14 (PDB id 1BQQ, [38]) and MMP-9 (PDB id: 1L6J, [39]) were gathered from the PDB-database (<http://www.rcsb.org/pdb/>). The Protein Preparation Wizard (Schrödinger Suite 2009 Protein Preparation Wizard; Epik version 2.0, Schrödinger, LLC, New York, NY, 2009; Impact version 5.5, Schrödinger, LLC, New York, NY, 2009; Prime version 2.1, Schrödinger, LLC, New York, NY, 2009) was used in processing of the proteins. Amino acids were deleted from 1L6J so that Phe107 became the N-terminal amino acid in accordance to what is seen in trypsin-activated MMP-9 [40], while TIMP-2 was removed from the 1BQQ complex. All water molecules except of those within 1 Å of the enzyme structure were removed. Het-states were generated (with metal mode), and the structures were minimized with an RMSD threshold of 0.30 Å relative to the starting structure (force field OPLS 2005). Glide integrated in the maestro interface was used for all steps in the docking and scoring (version 5.5, Schrodinger, LLC, New York, NY, 2009 [41–43]). For both structures a receptor grid was created with the active zinc as the centroid, allowing ligands of length up to 36 Å to be docked with default settings (corresponding to a $46 \times 46 \times 46 \text{ Å}^3$ grid). Docking was performed with standard precision and allowing 5–10 poses per ligand.

2.6. Synthesis, characterization and purification of PAC-1 and isatin derivatives

Compounds ISD-1, ISD-2, TZ-5, TZ-8 and TZ-11 were synthesized, characterized and purified as described previously [14]. For synthesis, characterization and purification of the various PAC-1 derivatives see supplementary data (Appendix A).

3. Results and discussion

3.1. Molecular modeling and docking of PAC-1 derivatives into the catalytic site of MMP-9 and MMP-14

PAC-1 derivatives that contain the central zinc chelating moiety *ortho*-hydroxy *N*-acyl hydrazine may bind to human MMPs by chelating the catalytic zinc. In the present study we have therefore docked six PAC-1 compounds containing the *ortho*-hydroxy *N*-acyl hydrazine moiety (Fig. 1) into the catalytic site of MMP-9 and MMP-14. The structural difference between the tested PAC-1 derivatives was the group attached at the R_1 , R_2 and R_3 positions of the benzene ring (Fig. 1).

The docking studies indicated that the compounds may bind to MMP-9 and MMP-14 and have several putative positions at the active sites with almost equivalent scoring values. However, it was not possible to rank the different poses relative to each other. This could be attributed to the combination of a flexible and relatively symmetric ligand with an open target site. The derivatives can either orient both the carbonyl oxygen and the phenol oxygen towards the zinc-ion of MMP-9 and MMP-14 as shown for PAC-1 in Fig. 2, or only the phenol

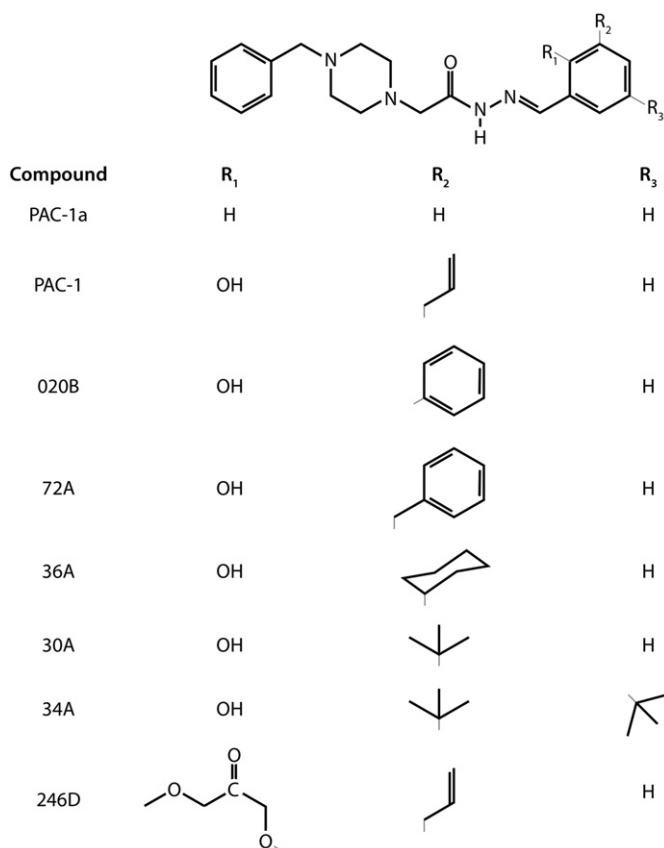


Fig. 1. Structure of the PAC-1 derivatives used in this article.

oxygen (not shown). In the poses with the latter orientation, the carbonyl-group was found at a larger distance to the zinc, and thus contributed less to zinc-binding. Most of the PAC-1 poses had the benzylpiperazine-group binding within the S1' pocket of the MMP-9, while in MMP-14, both oxygen atoms were mostly targeting the catalytic zinc and the R_2 group was targeting the S1' pocket. However, we cannot conclude that other poses of the PAC-1 derivatives are not possible in these enzymes.

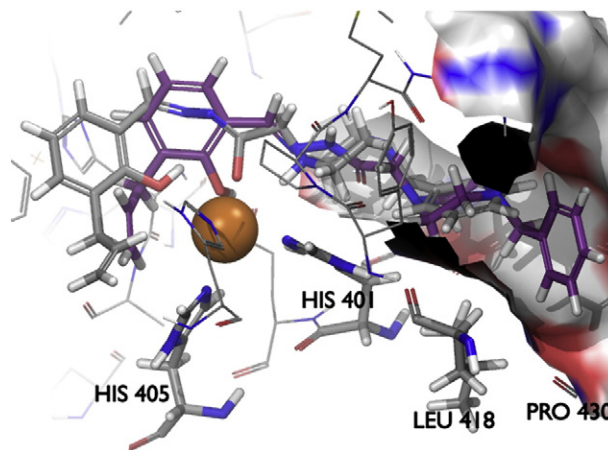


Fig. 2. PAC-1 docked into the active site of MMP-9. Two poses (purple and grey) of PAC-1 are shown as tube representation, with nitrogen atoms in blue and oxygen atoms in red. The three histidines coordinating the catalytic zinc (only two are labeled for simplicity) are shown. The grey surface represents a part of the S1' pocket with blue and red color representing positively and negatively charged regions, respectively. Leu418 and Pro430 are located in the S1' pocket. Both Maestro and Pymol (The PyMOL Molecular Graphic System, Version 1.5.0.4 Schrödinger, LLC) were used to generate the illustration.

3.2. Inhibitory effect of the PAC-1 derivatives against MMP-9 and MMP-14

To determine if some of the PAC-1 derivatives were strong inhibitors of MMP-9 and MMP-14, their inhibitory effect at 1.0 μM was tested, using 5.0 μM of the quenched fluorescence substrate McaPLGDpaAR. This substrate concentration is similar to the K_m values for the enzymes during the conditions used, which was $4 \pm 1 \mu\text{M}$ for MMP-9 and $6 \pm 1 \mu\text{M}$ for MMP-14. The enzyme reaction was started by adding enzyme to the mixture of inhibitor and substrate. No inhibition was observed with 1 μM of the PAC-1 derivatives. To determine whether these derivatives were slow tight binders, MMP-14 was incubated in the presence of 1.0 μM 020B for 0–60 min, and samples were withdrawn every 15 min and the activity was measured by adding the substrate (5.0 μM in assay). No time dependent inhibition was detected (data not shown) and hence it can be concluded that these derivatives are not slow tight binders of the MMPs.

The inhibitory power of 100 μM of the PAC-1 derivatives was then investigated. As shown in Fig. 3, more than 50% inhibition occurred for all derivatives except for PAC-1a and 246D which both lack the OH-group at the R_1 position (Fig. 1). In the docking studies, this OH-group was suggested to be involved in the binding to zinc in the active site (Fig. 2).

3.3. PAC-1 derivatives quench the formed fluorescence product of the peptide substrate McaPLGDpaAR

In the initial experiments it was discovered that the various PAC-1 derivatives gave background fluorescence at the wavelength used. Therefore we decided to determine to which extent the various PAC-1 derivatives also could quench the fluorescence of the formed product in the enzymatic reaction. These experiments were performed as described in the Materials and methods section, and we varied the concentration of the fluorescent product (McaPL-OH) in the absence and presence of different concentrations of the PAC-1 derivatives as shown in Fig. 4a for 020B. Because the PAC-1 derivatives had an own fluorescence, it was necessary to use various concentrations of McaPL-OH in the quenching experiments. This will mimic an initial rate curve, with

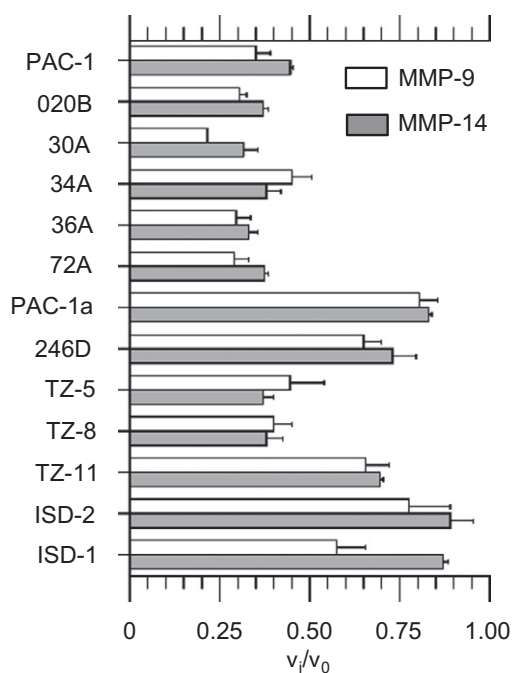


Fig. 3. Inhibitory effect of 100 μM PAC-1 and isatin derivatives on the activity of MMP-9 and MMP-14. The inhibition experiments were performed as described in Materials and methods, with a fixed concentration of the McaPLGDpaAR substrate.

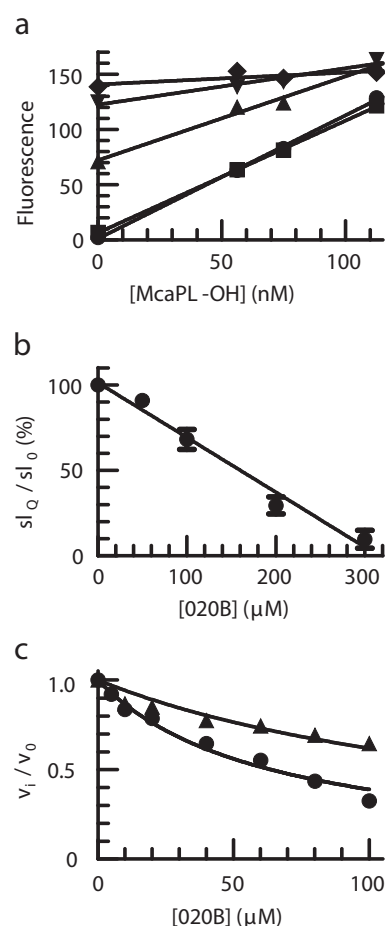


Fig. 4. Quenching and IC_{50} determination of the PAC-1 derivative 020B. (a) Primary quenching plots showing increasing fluorescence with increasing concentrations of the fluorescence product McaPL-OH in the presence of 0 (\bullet), 50 (\blacksquare), 100 (\blacktriangle), 200 (\blacktriangledown) and 300 μM (\blacklozenge) 020B. (b) Secondary plot where slopes in (a) are presented in % relative to unquenched curve (sl_Q/sl_0) and plotted against [020B] as described in Materials and methods. (c) Dose response plot of 020B for MMP-14 using the peptide substrate McaPLGDpaAR where v_i and v_0 are the initial rate in the presence and absence of 020B, respectively. Dose response curves where v_i was (\blacktriangle) and was not (\bullet) corrected for quenching.

increasing fluorescence with time due to the degradation of the fluorescence quenched substrate and the release of the Mca-fluorescence product. We determined to which extent the slope of the curves of [McaPL-OH] vs fluorescence decreased in the presence of PAC-1 derivatives as shown in Fig. 4a. A replot of the slopes of these curves against [020B] gave a linear curve $y = a_1x + b$ (Fig. 4b), with a slope a_1 (relative quenching coefficient) as presented in Table 1. The exception was for 72A, where the replot of slopes against [72A] gave an exponential

Table 1

IC_{50} values and quenching constants for PAC-1 and isatin derivatives. The quenching constant a_1 and the uncorrected and quench corrected IC_{50} values were obtained as described in methods. The quench constants a_1 was obtained from linear quench replots as shown in Fig. 4, while a_1^d for 72A was obtained from an exponential quenching curve as shown in the supplementary figure (Appendix B). N.I., no inhibition.

Compound	Quench constant a_1 (%/ μM)	MMP-9		MMP-14	
		IC_{50} (μM)		IC_{50} (μM)	
		Uncorr	Corr	Uncorr	Corr
020B	-0.32 ± 0.03	48 ± 3	112 ± 10	64 ± 3	163 ± 12
72A	-0.012 ± 0.001^a	78 ± 4	N.I.	71 ± 3	N.I.
TZ-5	-0.14 ± 0.02	126 ± 5	274 ± 23	126 ± 9	265 ± 36
TZ-8	-0.096 ± 0.006	160 ± 15	279 ± 32	190 ± 15	384 ± 29

quenching curve $y = b \times e^{-a_1x}$ (see Appendix B) with the quenching coefficient a_1 (Table 1).

No quenching of the DQ-gelatin fluorescence occurred in the presence of 100 μM of the two PAC-1 derivatives 020B and 72A. However at 300 μM , both PAC-1 derivatives started to quench.

3.4. IC_{50} determination of PAC-1 derivatives against MMP-9 and MMP-14

The molecular docking experiments along with the initial inhibitory experiments indicated that the various PAC-1 derivatives bind to the active site and inhibit the activity of both MMP-9 and MMP-14, and that the *ortho*-hydroxy *N*-acyl hydrazine moiety could chelate the catalytic zinc. To determine the binding strength of the PAC-1 derivatives for the two MMPs, IC_{50} values for the compounds were determined using a fixed concentration of the quenched fluorescence substrates McaPLGDpaAR (5 μM) and DQ-gelatin (4 $\mu\text{g}/\text{ml}$; 40 nM). These concentrations are similar to the obtained K_m values for the two enzymes. Hence, the obtained IC_{50} value should be approximately twice the K_i value for a competitive inhibitor. Fig. 4c shows a typical dose response plot for the compound 020B against MMP-14 using the small peptide substrate McaPLGDpaAR. If not correlated for quenching, an IC_{50} value of $64 \pm 3 \mu\text{M}$ was determined. When the v_i/v_0 values were corrected for quenching an IC_{50} value of $163 \pm 12 \mu\text{M}$ was obtained (Fig. 4c). Curves similar to that in Fig. 4c were also obtained for the PAC-1 derivatives 020B and 72A against both MMP-9 and MMP-14 (Table 1). In all cases when v_i/v_0 results had been corrected for quenching, the IC_{50} values were well above 100 μM . This reveals that the PAC-1 derivatives used are only weak inhibitors of these two MMPs and it can also be assumed that other PAC-1 derivatives are weak MMP-9 and MMP-14 inhibitors. Since the active site of the various MMPs appears to be similar, we can also assume that PAC-1 and its derivatives have weak binding affinities to the active site of other MMPs.

In order to test whether the obtained inhibitory results with the PAC-1 derivatives against the small fluorescence quenched peptide substrate McaPLGDpaAR also is valid against more biological substrates we have tested if 020B and 72A inhibit the MMP-9 degradation of DQ-gelatin.

In contrast to the degradation of small peptide substrates like McaPLGDpaAR, degradation of gelatin by MMP-9 is dependent on an intact F_{NI} module which acts as an exosite. Furthermore, proMMP-9 binds to gelatin through the F_{NI} module which has been exploited in the purification of the enzyme [35,44,45]. Previously we showed that approximately 50% of proMMP-9 bound to gelatin coated microplates was released when 0.9% DMSO was added [35]. We therefore tested to which extent DMSO affected the MMP-9 degradation rate of both DQ-gelatin and McaPLGDpaAR. As shown in Fig. 5(a), there are large differences in the effect of DMSO on the MMP-9 degradation rate of DQ-gelatin and McaPLGDpaAR. In the presence of 0.72% of DMSO, a 50% decrease in degradation rate of DQ-gelatin occurred, while the degradation of McaPLGDpaAR was unaffected. This fits well with a previous work [46]. In the presence of 5% DMSO, only 5% of the activity against DQ-gelatin remained, while approximately 40% remained in the presence of 1% DMSO. As it was possible to dissolve 100 μM of the two PAC-1 derivatives 020B and 72A in the Hepes buffer containing 1% DMSO, this assay condition was used for the inhibition experiments with DQ-gelatin. A K_m value of $3.9 \pm 0.5 \mu\text{g}/\text{ml}$ ($39 \pm 5 \text{ nM}$) was obtained in the presence of 1% DMSO and $3.9 \pm 0.4 \mu\text{g}/\text{ml}$ in the absence of DMSO. Thus, the presence of this DMSO concentration did not affect the K_m value but the catalytic efficiency of the enzyme. In order to compare the results from the assay with McaPLGDpaAR substrate, 40 nM of DQ-gelatin which is similar to the K_m value was used in these inhibition experiments. As expected, almost no inhibition was obtained with 72A, while a slight inhibition occurred with 020B (Fig. 5(b)). The estimated IC_{50} value for the latter compound was $238 \pm 30 \mu\text{M}$. This value is approximately twice as high as the estimated value against the McaPLGDpaAR substrate after corrections for quenching, which is a

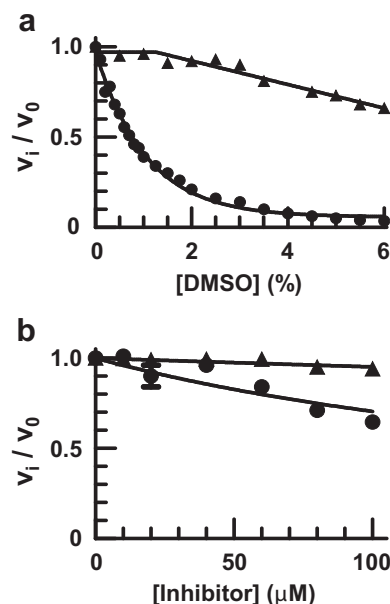


Fig. 5. DMSO inhibition of MMP-9 activity and dose response plots of 020B and 72A for MMP-9 using DQ-gelatin. (a) Dose response plot showing the inhibitory effect of DMSO on the MMP-9 activity against 4.0 $\mu\text{g}/\text{ml}$ DQ-gelatin (●) and 5.0 μM McaPLGDpaAR (▲). (b) Dose response plot of 020B (●) and 72A (▲) for MMP-9 using DQ-gelatin and a buffer containing 1% DMSO as described in Materials and methods. The initial rates v_i and v_0 are in the presence and absence of inhibitor, respectively.

good correlation due to the circumstances with inhibitor solubility and the effect of DMSO on the DQ-gelatin assay. Overall, these results show that the PAC-1 derivatives are not only weak inhibitors against MMP-9 degradation of the fluorescence-quenched small peptide substrate McaPLGDpaAR, but also against the physiological substrate gelatin.

PAC-1 derivatives induced apoptosis in various cell lines by activation of procaspase-3 and -7 [7–10]. Although the K_d values for zinc-binding of the PAC-1 derivatives were in the lower to middle nM region, the concentration needed to induce apoptosis in U-937 cells was in the lower μM region (1–4 μM) [8]. Furthermore, PAC-1 concentrations from 0.003 to 1.4 μM induced apoptosis in various types of cancer cells depending on their level of procaspase-3 [11]. Those PAC-1 derivatives that lacked an OH-group at the R_1 position had a much weaker zinc binding capacity, did not activate procaspase-3 and needed much higher concentrations to induce apoptosis in U-937 cells [10]. The concentration that induced apoptosis by the PAC-1 derivatives with an OH-group at the R_1 position had no or only minor inhibitory effect on MMP-9 and MMP-14. This could be beneficial due to the dual effects these MMPs exert with respect to apoptotic cell death, cell survival and homeostasis.

3.5. Molecular modeling and docking of isatin derivatives into the catalytic site of MMP-9 and MMP-14

The isatin derivatives used in this docking study are shown in Fig. 6.

The compounds have two carbonyl groups on the indole core, and for ISD-1 the docking suggested that one of the carbonyl oxygen atoms forms a mono-dentate interaction with the zinc-ion in MMP-9. This carbonyl is conjugated to nitrogen. The structurally identical parts of ISD-1, TZ-5 and TZ-8 showed similar poses within MMP-9. The size of the R_2 -chain of these compounds is varying, and this chain protrudes to different degrees into the S1'-pocket as shown in Fig. 7. ISD-1 with the smallest R_2 -chain interacted only with amino acids lining and defining the opening of the S1'-pocket. TZ-5 goes deeper into the pocket and established additional interactions, while TZ-8 interacts favorably with amino acids at the bottom of the pocket (Fig. 7). TZ-8 also adapted a

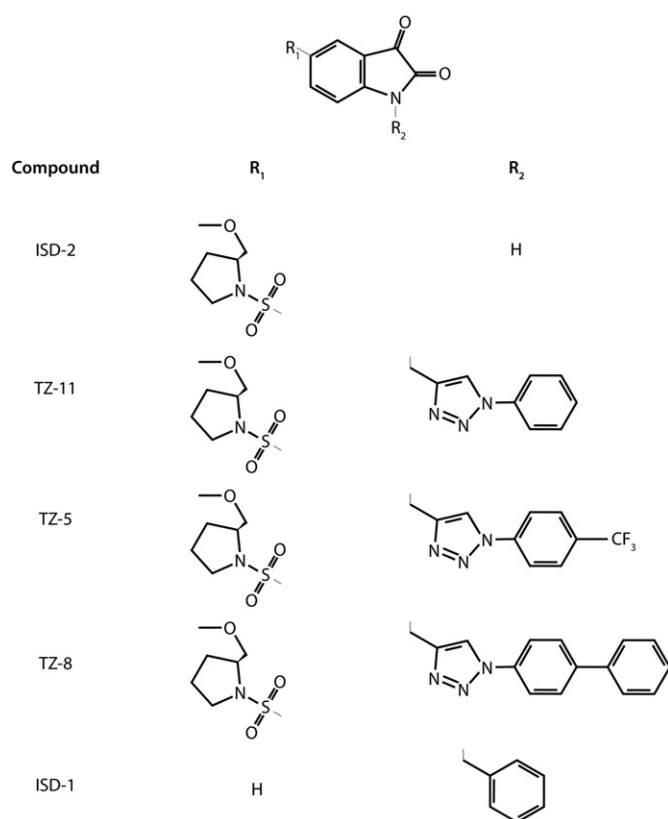


Fig. 6. Structure of the isatin derivatives used in this article.

similar position within MMP-14, while TZ-5 preferred a different position in MMP-14 (not shown).

3.6. Inhibitory effect of the isatin derivatives against MMP-9 and MMP-14

To determine if some of the isatin derivatives were strong inhibitors of MMP-9 and MMP-14, their inhibitory effect at 1.0 μM was first tested, using 5.0 μM of the quenched fluorescence substrate McaPLGDpaAR as described for the PAC-1 derivatives. No inhibition was observed at this concentration and furthermore, no time dependent inhibition was

detected using TZ-5. This suggests that neither of these derivatives is a strong or tight slow binder of the MMPs.

Next the inhibitor effect of 100 μM of the isatin derivatives was investigated. As shown in Fig. 3, more than 50% inhibition occurred only for TZ-5 and TZ-8. The inhibition was much less for the other three derivatives (TZ-11, ISD-1 and ISD-2).

3.7. Isatin derivatives quench the formed fluorescence products of McaPLGDpaAR and DQ-gelatin

As for the PAC-1 derivatives, the isatin derivatives also have intrinsic fluorescence at the wavelength used with the small peptide substrate McaPLGDpaAR. To determine if these derivatives also quench the detection of the MMP reaction, quenching studies were performed as described for the PAC-1 derivatives. The a_1 values for the secondary quenching curves with slopes against [isatin derivatives] are presented in Table 1. In contrast to the PAC-1 derivatives, TZ5 and TZ8 were strong quenchers of the fluorescence generated from the cleavage of DQ-gelatin.

3.8. IC₅₀ determination of isatin 1,2,3-triazole derivatives against MMP-9 and MMP-14

The strength of the interaction between the two isatin 1,2,3-triazole derivatives TZ-5 and TZ-8 and the two metalloproteinases MMP-9 and MMP-14 was determined. The two tested compounds were weak inhibitors against both enzymes with IC₅₀ values larger than 100 μM after quenching corrections (Table 1). This suggests that also the other isatin derivatives studied in this work are only weak inhibitors of MMPs. Due to quenching these compounds were not tested against MMP-9 degradation of DQ-gelatin.

When the cellular concentration of mobile zinc has been largely reduced, an uncontrolled activation of the executioner caspases-3 and -7 occurs followed by apoptosis [47]. Dysregulation of apoptotic cell death has been observed in a large number of pathological conditions such as airway inflammation and asthma, type-1 diabetes, ischemia-reperfusion (stroke and myocardial infarction), cardiomyopathy, sepsis and neurodegeneration (Alzheimer's disease, Parkinson's disease, Huntington's disease, ALS) [14,47–50]. Under such circumstances it may be beneficial to inhibit the activation and activity of the executioner caspases. For that purpose a number of isatin derivatives have been developed that inhibits caspase-3 and -7 with IC₅₀ values in the lower nM region. The isatin 1,2,3-triazoles are among these compounds [12–14]. TZ-5, -8 and -11 inhibited caspase-3 with IC₅₀ values around 20 nM using an *in vitro* assay [14]. When IC₅₀ values for caspase-3 were determined both *in vitro* and in whole cells, the latter assay gave 10–100 times higher values [12]. Some isatin derivatives that inhibited caspase-3 with IC₅₀ values between 3 and 40 nM *in vitro* gave good protection against apoptosis of Jurkat and chondrocyte cells using a concentration of 10 μM [51]. The present work shows that at the concentrations of the isatin derivatives needed to inhibit the caspases in the cells are far lower than the IC₅₀ values for MMP inhibition, enzymes which are localized outside the cells. As for the PAC-1 derivatives, one can assume that the concentrations used of the isatin derivatives to inhibit the caspases and protect cells from apoptosis are too low to affect the activity of MMPs. Therefore, unwanted side effects from inhibition of MMPs are not likely to occur.

4. Concluding remarks

In this work we have investigated to which extent caspase activators (PAC-1 derivatives) and inhibitors (isatin derivatives) affect the activity of MMPs. Our findings show that none of these compounds are strong MMP inhibitors. This suggests that the development and use of caspase activators and inhibitors based on the compounds studied in the

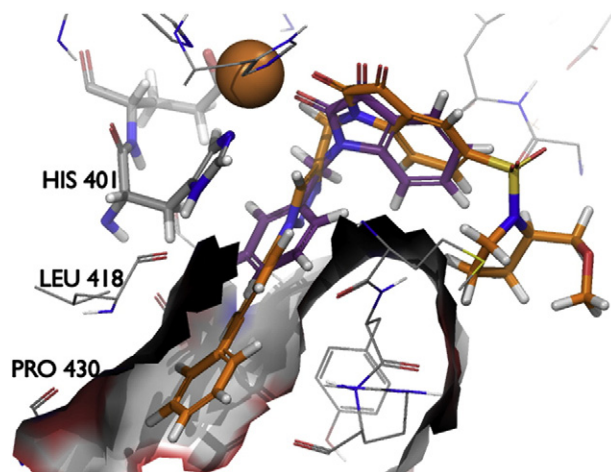


Fig. 7. ISD-1 and TZ-8 docked into the active site of MMP-9. ISD-1 (purple carbon chain) and TZ-8 (orange carbon chain) are shown as tube representation. The three histidines (one is labeled) coordinating the zinc (in gold) are shown. The grey surface represents part of the S1' pocket, with positively and negatively charged regions in blue and red, respectively. Leu480 and Pro430 are located in the S1'-pocket. The figure was generated with Maestro and Pymol.

present work would not give rise to unwanted effects through inhibition of MMPs.

Supplementary data to this article can be found online at <http://dx.doi.org/10.1016/j.bbagen.2014.07.011>.

Author's contributions

Designed and prepared the PAC-1 derivatives: TVH and ØWA. Designed and prepared the isatin derivatives: TVH and JY. Designed and performed molecular modeling and docking experiments: IS and SS. Performed production, purification and activation of proMMP-9: EB. Designed and performed kinetic and inhibition experiments JOW, SS, and AIS. Designed and performed quenching experiments: JOW and AIS. Contributed reagents/materials/analysis tools: JOW, TVH, and IS. Wrote and revised the paper: JOW, IS, TVH, SS, AIS, ØWA, EB, and JY.

Acknowledgments

This work was in part supported by grants from the Norwegian Cancer Society, the Erna and Olav Aakre Foundation for Cancer, Tromsø Forskningsstiftelse and The Research Council of Norway (KOSK-II 185222). We also would like to thank Rod Wolstenholme (Faculty of Health Sciences, UiT-The Arctic University of Norway) for help with the drawing of Figs. 1 and 6.

References

- [1] P.J. Polverini, J.E. Nor, Apoptosis and predisposition to oral cancer, *Crit. Rev. Oral Biol. Med.* 10 (1999) 139–152.
- [2] A. Barzilai, DNA damage, neuronal and glial cell death and neurodegeneration, *Apoptosis* 15 (2010) 1371–1381.
- [3] J. Zivny, P. Kleiner Jr., R. Pytlík, L. Andera, The role of apoptosis in cancer development and treatment: focusing on the development and treatment of hematologic malignancies, *Curr. Pharm. Des.* 16 (2010) 11–33.
- [4] D. Hanahan, R.A. Weinberg, The hallmarks of cancer, *Cell* 100 (2000) 57–70.
- [5] C.M. Troy, N. Akpan, Y.Y. Jean, Regulation of caspases in the nervous system implications for functions in health and disease, *Prog. Mol. Biol. Transl. Sci.* 99 (2011) 265–305.
- [6] P. Hensley, M. Mishra, N. Kyprianou, Targeting caspases in cancer therapeutics, *Biol. Chem.* 394 (2013) 831–843.
- [7] G. Aziz, O.W. Akselsen, T.V. Hansen, R.E. Paulsen, Procaspase-activating compound 1 induces a caspase-3-dependent cell death in cerebellar granule neurons, *Toxicol. Appl. Pharmacol.* 247 (2010) 238–242.
- [8] D.C. Hsu, H.S. Roth, D.C. West, R.C. Botham, C.J. Novotny, S.C. Schmid, P.J. Hergenrother, Parallel synthesis and biological evaluation of 837 analogues of procaspase-activating compound 1 (PAC-1) and its cellular co-localization with caspase-3, *J. Med. Chem.* 52 (2009) 5721–5731.
- [9] Q.P. Peterson, D.R. Goode, D.C. West, K.N. Ramsey, J.J. Lee, P.J. Hergenrother, PAC-1 activates procaspase-3 in vitro through relief of zinc-mediated inhibition, *J. Mol. Biol.* 388 (2009) 144–158.
- [10] Q.P. Peterson, D.C. Hsu, D.R. Goode, C.J. Novotny, R.K. Totten, P.J. Hergenrother, Procaspase-3 activation as an anti-cancer strategy: structure-activity relationship of procaspase-activating compound 1 (PAC-1) and its cellular co-localization with caspase-3, *J. Med. Chem.* 52 (2009) 5721–5731.
- [11] K.S. Putt, G.W. Chen, J.M. Pearson, J.S. Sandhorst, M.S. Hoagland, J.T. Kwon, S.K. Hwang, H. Jin, M.I. Churchwell, M.H. Cho, D.R. Doerge, W.G. Helferich, P.J. Hergenrother, Small-molecule activation of procaspase-3 to caspase-3 as a personalized anticancer strategy, *Nat. Chem. Biol.* 2 (2006) 543–550.
- [12] W. Chu, J. Rothfuss, D. Zhou, R.H. Mach, Synthesis and evaluation of isatin analogs as caspase-3 inhibitors: introduction of a hydrophilic group increases potency in a whole cell assay, *Bioorg. Med. Chem. Lett.* 21 (2011) 2192–2197.
- [13] W. Chu, J. Zhang, C. Zeng, J. Rothfuss, Z. Tu, Y. Chu, D.E. Reichert, M.J. Welch, R.H. Mach, N-benzylisatin sulfonamide analogues as potent caspase-3 inhibitors: synthesis, in vitro activity, and molecular modeling studies, *J. Med. Chem.* 48 (2005) 7637–7647.
- [14] Y. Jiang, T.V. Hansen, Isatin 1,2,3-triazoles as potent inhibitors against caspase-3, *Bioorg. Med. Chem. Lett.* 21 (2011) 1626–1629.
- [15] W. Bode, F.X. Gomis-Ruth, W. Stockler, Astacins, serralytins, snake venom and matrix metalloproteinases exhibit identical zinc-binding environments (HEXXHXXGXXH and Met-turn) and topologies and should be grouped into a common family, the 'metzincins', *FEBS Lett.* 331 (1993) 134–140.
- [16] E. Hadler-Olsen, B. Fadnes, I. Sylte, L. Uhlin-Hansen, J.O. Winberg, Regulation of matrix metalloproteinase activity in health and disease, *FEBS J.* 278 (2011) 28–45.
- [17] G.S. Butler, C.M. Overall, Updated biological roles for matrix metalloproteinases and new "intracellular" substrates revealed by degradomics, *Biochemistry* 48 (2009) 10830–10845.
- [18] C.R. Flannery, MMPs and ADAMTS: functional studies, *Front. Biosci.* 11 (2006) 544–569.
- [19] C. Gialeli, A.D. Theocharis, N.K. Karamanos, Roles of matrix metalloproteinases in cancer progression and their pharmacological targeting, *FEBS J.* 278 (2011) 16–27.
- [20] C.J. Malemud, Matrix metalloproteinases (MMPs) in health and disease: an overview, *Front. Biosci.* 11 (2006) 1696–1701.
- [21] H. Nagase, R. Visse, G. Murphy, Structure and function of matrix metalloproteinases and TIMPs, *Cardiovasc. Res.* 69 (2006) 562–573.
- [22] H.J. Ra, W.C. Parks, Control of matrix metalloproteinase catalytic activity, *Matrix Biol.* 26 (2007) 587–596.
- [23] R.J. Tan, Y. Liu, Matrix metalloproteinases in kidney homeostasis and diseases, *Am. J. Physiol. Ren. Physiol.* 302 (2012) F1351–F1361.
- [24] C. Arnould, M. Lelievre-Pegorier, P. Ronco, B. Lelongt, MMP9 limits apoptosis and stimulates branching morphogenesis during kidney development, *J. Am. Soc. Nephrol.* 20 (2009) 2171–2180.
- [25] S. Bengatta, C. Arnould, E. Letavernier, M. Monge, H.M. de Preneuf, Z. Werb, P. Ronco, B. Lelongt, MMP9 and SCF protect from apoptosis in acute kidney injury, *J. Am. Soc. Nephrol.* 20 (2009) 787–797.
- [26] T.M. Camp, S.C. Tyagi, R.M. Senior, M.R. Hayden, Gelatinase B(MMP-9) an apoptotic factor in diabetic transgenic mice, *Diabetologia* 46 (2003) 1438–1445.
- [27] J.C. Copin, M.C. Goodyear, J.M. Gidday, A.R. Shah, E. Gascon, A. Dayer, D.M. Morel, Y. Gasche, Role of matrix metalloproteinases in apoptosis after transient focal cerebral ischemia in rats and mice, *Eur. J. Neurosci.* 22 (2005) 1597–1608.
- [28] M. Fatunmbi, J. Shelton, S.M. Aronica, MMP-9 increases HER2/neu expression and alters apoptosis levels in human mammary epithelial cells (HMEC), *Breast Cancer Res. Treat.* 135 (2012) 519–530.
- [29] E. Kolaczowska, A. Koziol, B. Plytycz, B. Arnold, G. Opdenakker, Altered apoptosis of inflammatory neutrophils in MMP-9-deficient mice is due to lower expression and activity of caspase-3, *Immunol. Lett.* 126 (2009) 73–82.
- [30] R.A. Kowluru, G. Mohammad, J.M. dos Santos, Q. Zhong, Abrogation of MMP-9 gene protects against the development of retinopathy in diabetic mice by preventing mitochondrial damage, *Diabetes* 60 (2011) 3023–3033.
- [31] A.K. Nalla, B. Gorantla, C.S. Gondi, S.S. Lakka, J.S. Rao, Targeting MMP-9, uPAR, and cathepsin B inhibits invasion, migration and activates apoptosis in prostate cancer cells, *Cancer Gene Ther.* 17 (2010) 599–613.
- [32] M.H. Sun, K.J. Chen, Y.P. Tsao, L.Y. Kao, W.H. Han, K.K. Lin, J.H. Pang, Down-regulation of matrix metalloproteinase-9 by pyrrolidine dithiocarbamate prevented retinal ganglion cell death after transection of optic nerve in rats, *Curr. Eye Res.* 36 (2011) 1053–1063.
- [33] J. Xu, H. Liu, Y. Wu, X. Gong, Q. Zhou, F. Qiao, Proapoptotic effect of metalloproteinase 9 secreted by trophoblasts on endothelial cells, *J. Obstet. Gynaecol. Res.* 37 (2011) 187–194.
- [34] C.M. Yang, H.L. Hsieh, C.C. Lin, R.H. Shih, P.L. Chi, S.E. Cheng, L.D. Hsiao, Multiple factors from bradykinin-challenged astrocytes contribute to the neuronal apoptosis: involvement of astroglial ROS, MMP-9, and HO-1/CO system, *Mol. Neurobiol.* 47 (2013) 1020–1033.
- [35] N. Malla, E. Berg, L. Uhlin-Hansen, J.O. Winberg, Interaction of pro-matrix metalloproteinase-9/proteoglycan hateromer with gelatin and collagen, *J. Biol. Chem.* 283 (2008) 13652–13665.
- [36] J.O. Winberg, E. Berg, S.O. Kolset, L. Uhlin-Hansen, Calcium-induced activation and truncation of promatrix metalloproteinase-9 linked to the core protein of chondroitin sulfate proteoglycans, *Eur. J. Biochem.* 270 (2003) 3996–4007.
- [37] J.C. Shelley, A. Cholleti, L.L. Frye, J.R. Greenwood, M.R. Timlin, M. Uchimaya, Epik: a software program for pK(a) prediction and protonation state generation for drug-like molecules, *J. Comput. Aided Mol. Des.* 21 (2007) 681–691.
- [38] C. Fernandez-Catalan, W. Bode, R. Huber, D. Turk, J.J. Calvete, A. Lichte, H. Tschesche, K. Maskos, Crystal structure of the complex formed by the membrane type 1-matrix metalloproteinase with the tissue inhibitor of metalloproteinases-2, the soluble progelatinase A receptor, *EMBO J.* 17 (1998) 5238–5248.
- [39] S. Rowsell, P. Hawtin, C.A. Minshall, H. Jepson, S.M. Brockbank, D.G. Barratt, A.M. Slater, W.L. McPheat, D. Waterson, A.M. Henney, R.A. Pauptit, Crystal structure of human MMP9 in complex with a reverse hydroxamate inhibitor, *J. Mol. Biol.* 319 (2002) 173–181.
- [40] Q.X. Sang, H. Birkedal-Hansen, H.E. Van Wart, Proteolytic and non-proteolytic activation of human neutrophil progelatinase B, *Biochim. Biophys. Acta* 1251 (1995) 99–108.
- [41] R.A. Friesner, J.L. Banks, R.B. Murphy, T.A. Halgren, J.J. Klicic, D.T. Mainz, M.P. Repasky, E.H. Knoll, M. Shelley, J.K. Perry, D.E. Shaw, P. Francis, P.S. Shenkin, Glide: a new approach for rapid, accurate docking and scoring. 1. Method and assessment of docking accuracy, *J. Med. Chem.* 47 (2004) 1739–1749.
- [42] R.A. Friesner, R.B. Murphy, M.P. Repasky, L.L. Frye, J.R. Greenwood, T.A. Halgren, P.C. Sanschagrin, D.T. Mainz, Extra precision glide: docking and scoring incorporating a model of hydrophobic enclosure for protein-ligand complexes, *J. Med. Chem.* 49 (2006) 6177–6196.
- [43] T.A. Halgren, R.B. Murphy, R.A. Friesner, H.S. Beard, L.L. Frye, W.T. Pollard, J.L. Banks, Glide: a new approach for rapid, accurate docking and scoring. 2. Enrichment factors in database screening, *J. Med. Chem.* 47 (2004) 1750–1759.
- [44] G. Murphy, T. Crabbe, Gelatinases A and B, *Methods Enzymol.* 248 (1995) 470–484.
- [45] X. Xu, Z. Chen, Y. Wang, Y. Yamada, B. Steffensen, Functional basis for the overlap in ligand interactions and substrate specificities of matrix metalloproteinases-9 and -2, *Biochem. J.* 392 (2005) 127–134.
- [46] J. Vandoren, N. Geurts, E. Martens, P.E. Van den Steen, S.D. Jonghe, P. Herdewijn, G. Opdenakker, Gelatin degradation assay reveals MMP-9 inhibitors and function of O-glycosylated domain, *World J. Biol. Chem.* 2 (2011) 14–24.
- [47] A.Q. Truong-Tran, D. Grosser, R.E. Ruffin, C. Murgia, P.D. Zalewski, Apoptosis in the normal and inflamed airway epithelium: role of zinc in epithelial protection and procaspase-3 regulation, *Biochem. Pharmacol.* 66 (2003) 1459–1468.

- [48] U. Fischer, K. Schulze-Osthoff, New approaches and therapeutics targeting apoptosis in disease, *Pharmacol. Rev.* 57 (2005) 187–215.
- [49] J.C. Reed, Apoptosis-based therapies, *Nat. Rev. Drug Discov.* 1 (2002) 111–121.
- [50] I. Rodríguez, K. Matsuura, C. Ody, S. Nagata, P. Vassalli, Systemic injection of a tripeptide inhibits the intracellular activation of CPP32-like proteases in vivo and fully protects mice against Fas-mediated fulminant liver destruction and death, *J. Exp. Med.* 184 (1996) 2067–2072.
- [51] D. Lee, S.A. Long, J.H. Murray, J.L. Adams, M.E. Nuttall, D.P. Nadeau, K. Kikly, J.D. Winkler, C.M. Sung, M.D. Ryan, M.A. Levy, P.M. Keller, W.E. DeWolf Jr., Potent and selective nonpeptide inhibitors of caspases 3 and 7, *J. Med. Chem.* 44 (2001) 2015–2026.